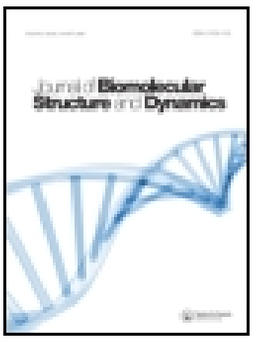

Taylor & Francis
Taylor & Francis Group

Journal of Biomolecular Structure and Dynamics

ISSN: (Print) (Online) Journal homepage: https://www.tandfonline.com/loi/tbsd20

Theoretical-experimental studies of calmodulin-peptide interactions at different calcium equivalents

Alejandro Sosa-Peinado , Erika León-Cruz , Isabel Velázquez-López , Deyamira Matuz-Mares , Patricia Cano-Sánchez & Martin González-Andrade

To cite this article: Alejandro Sosa-Peinado , Erika León-Cruz , Isabel Velázquez-López , Deyamira Matuz-Mares , Patricia Cano-Sánchez & Martin González-Andrade (2020): Theoretical-experimental studies of calmodulin-peptide interactions at different calcium equivalents, Journal of Biomolecular Structure and Dynamics, DOI: 10.1080/07391102.2020.1841679

To link to this article: https://doi.org/10.1080/07391102.2020.1841679

JOURNAL OF BIOMOLECULAR STRUCTURE AND DYNAMICS
https://doi.org/10.1080/07391102.2020.1841679

Theoretical-experimental studies of calmodulin-peptide interactions at different calcium equivalents

Alejandro Sosa-Peinado[a], Erika León-Cruz[a], Isabel Velázquez-López[a], Deyamira Matuz-Mares[a], Patricia Cano-Sánchez[b] and Martin González-Andrade[a]

[a]Facultad de Medicina, Universidad Nacional Autónoma de México, Ciudad de México, México; [b]Instituto de Química, Universidad Nacional Autónoma de México, Ciudad de México, México

Communicated by Ramaswamy H. Sarma

ABSTRACT

We study the CaM-peptide interactions for four CaM-related peptides with different calcium equivalents, using the *h*CaM-M124C-*mBBr* biosensor and Molecular Dynamics (MD). Due to the high sensitivity of the biosensor, we were able to calculate five K_{ds} based on the number of calcium equivalents for each peptide, showing a directly proportional relationship between the degree of calcium saturation and the increased affinity for the Calspermin, nNOS, and skMLSK peptides; while the CaV1.1 peptide has a degree of affinity independent of the number of calcium equivalent. On the other hand, the MD studies were designed based on the experimental results; I) visualizing the effect of the gradual elimination of calcium in Holo-CaM and II) analyzing the CaM-Peptide complexes with and without calcium. We observe that the gradual addition of calcium increases the flexibility of Holo-CaM. Concerning CaM-Peptide complexes, it presents differences in both the ΔG_T and the RMSD. These results demonstrate the importance of the use of biosensors and the power of MD to make inferences in systems such as CaM-peptide complexes.

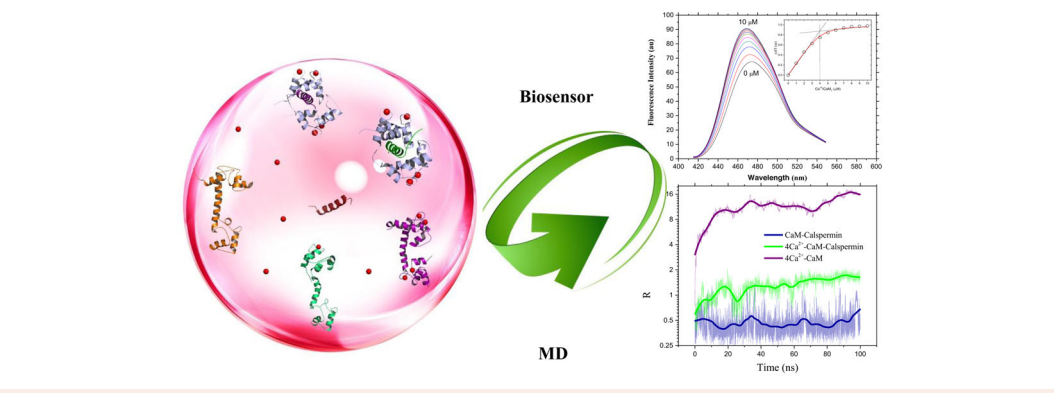

ARTICLE HISTORY
Received 8 August 2020
Accepted 20 October 2020

KEYWORDS
CaM-peptide; molecular modeling tools; calcium; molecular dynamic (MD); biosensors; calmodulin; calspermin; CaV1.1; nNOS; and skMLCK

1. Introduction

The calcium ion (Ca^{+2}) plays an essential role in the physiology of higher organisms after activating multiple signaling cascades to respond to changes in the environment and maintain cellular homeostasis; regulating processes such as exocytosis, muscle contraction, gene transcription, energy metabolism, cell proliferation, among the most critical (Audran et al., 2013; Berridge, 1997; Brini & Carafoli, 2000). The physiological concentration of free intracellular Ca^{+2} is strictly controlled. It is usually lower in the cytosol (~0.1-20 μM) than the concentration of extracellular, being approximately three orders of magnitude greater ~100-1000 μM -subcellular organelles and extracellular matrix (Vetter & Leclerc, 2003).

Calmodulin (CaM) is a ubiquitous protein, highly conserved, and considered the main calcium signaling protein in eukaryotic cells. This protein controls various physiological processes such as cell motility, cytoskeleton architecture and function, cell proliferation, apoptosis, autophagy, ion transport, osmotic control, protein phosphorylation/dephosphorylation, reproductive processes, muscle contraction, and gene expression (Mata et al., 2015; O'Day, 2003). CaM is a small, acidic protein comprising of 148 amino acids (16.7 kDa) (Ishida & Vogel, 2006). Interacts and

CONTACT Martin González-Andrade martin@bq.unam.mx Facultad de Medicina, Universidad Nacional Autónoma de México, Ciudad de México C.P 04510, México

Supplemental data for this article can be accessed online at https://doi.org/10.1080/07391102.2020.1841679.

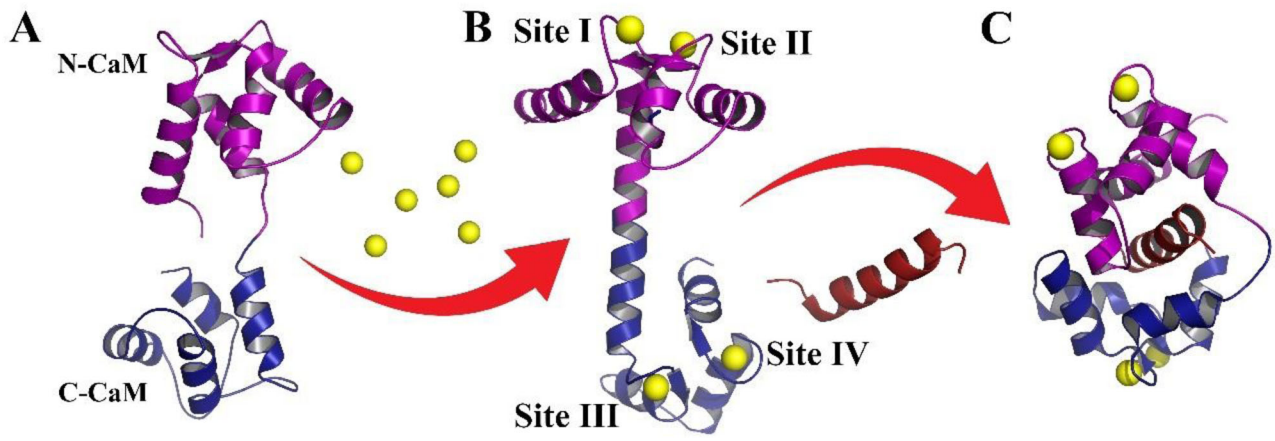

Figure 1. Three-dimensional structures of the CaM. A) Apo-CaM, shown in purple cartoons, the N-Terminal domain (N-CaM), and in blue cartoons, the C-Terminal domain, this structure was solved by NMR (ICFD.pdb) (Kuboniwa et al., 1995). B) Holo-CaM, shows the four calcium-binding sites, the site I and II correspond to the N-CaM domain (higher affinity) and site III and IV to the C-CaM domain (lower affinity), the structure was resolved by X-Ray diffraction (1CLL.pdb) (Chattopadhyaya et al., 1992). Ca-CaM-peptide nNOS complex, a peptide shown in red wine caricature, solved by X-Ray diffraction (2O60.pdb).

Table 1. Shows some CaM-binding peptides, representing the region of the different proteins with which CaM interacts.

Motive	Name	Sequence	PDB	Ref.
1-5-10	CaMKI	————IKKNFAKSKWKQAFNATAVVRHMRK————	1MXE	(Clapperton et al., 2002)
	CaMKII	————LKKFNARRKLKGAILTTMLATRNFS————	1CM1	(Wall et al., 1997)
	skMLCK	————KRRWKKNFIAVSAANRFKKISSSGAL————	2LV6	(Grishaev et al., 2012)
1-8-14	smMLCK	————ARRKWQKTGHAVRAIGRLSS————————	1CDL	(Meador et al., 1992)
	DAPK-1	————RRRWKLDFSIVSLCNHLTR————————	1ZUZ	–
	nNOS	————KRRAIGFKKLAEAVKFSAKLMGQ————————	2O60	–
1-5-8-14	Calcineurin	————ARKEVIRNKIRAIGKMARVFSVLR————————	2JZI	–
	Calspermin	————ARRK-LKAAVKAVVASSRLGS————————	*	–
1-17	Ryanodine-1 receptor	————KSKKAVWHKLLSKQRRRAVVACFRMTPLYN-	2BCX	(Maximciuc et al., 2006)
1-7-10	NMDA receptor	————KKKATFRAITSTLASSFKRRRSSK————————	2HQW	(Ataman et al., 2007)
1-10	Cav1.1	——————KFYATFLIQEHFRKFMKRQEE————————	2VAY	(Halling et al., 2009)
	Cav1.2	GHMDEVTVGKFYATFLIQEYFRKFKKRKEQGLVGKPS	2BE6	(Van Petegem et al., 2005)
1-5-8	PMCA	————LRRGQILWFRGLNRIQTQIK————————	1CFF	(Elshorst et al., 1999)
IQ	Neuromodulin	————AATKIQASFRGHITRKKLKGEKKG————————	*	–
	Neurogranin	——NAAAAKIQASFRGHMARKKIKSGE————————	*	–
Otros	Citropin 1.1	——————————GLFDVIKKVASVIKKL————————————	*	–
	Aurein 2.3	——————————GLFDIVKKVVGIAGSL————————————	*	–
	Dahlein 5.6	——————————GLLASLGKVFGGYLAEKLKPK————————	*	–

regulates multiple proteins across its two globular domains called "EF-hand". Each domain has two Ca^{+2} binding sites; the C-terminal lobe has a high binding affinity for Ca^{+2}, K_d = 0.2 μM, and the N-terminal lobe a K_d = 2 μM (Vetter & Leclerc, 2003). CaM can be found in three main conformations depending on ligand binding: A) Apo-CaM conformation, when CaM is in the absence of calcium (Jurado et al., 1999), B) Holo-CaM, after binding of Ca^{+2} ions the protein shows conformational changes; their alpha-helices from EF-hand domains adopt an almost perpendicular conformation, this conformation is also called an open conformation (Komeiji et al., 2002), and C) Closed conformation when CaM interacts with different ligands such as proteins, peptides or drugs (Figure 1).

CaM modulates a wide variety of proteins; these are involved in cell growth, phosphorylation, dephosphorylation, replication, transcription, cellular metabolism of calcium, and second messengers, among the most important (Mata et al., 2015). Based on CaM-protein interactions, a wide variety of peptides have been reported that interact and inhibit CaM. Table 1 shows some CaM-binding peptides, representing the region of the different proteins with which CaM interacts. The structures of the CaM-peptide complexes show interactions in the hydrophobic areas of the CaM protein in the same way as the classic proteins and inhibitors reported (Rhoads & Friedberg, 1997); peptides possess a positively charged amphiphilic alpha-helical structure, regardless of their amino acid sequences (O'Neil & DeGrado, 1990). These peptides have affinities (K_d) in the order of 10^{-9}–10^{-12} M, being comparable to or better than the proteins that precede them and more significant than that of classic organic CaM inhibitors (10^{-3} M) (Chen et al., 2016; Peersen et al., 1997). Thus, they can potentially be considered as bioactive molecules, as they are biological molecules with a high affinity for CaM capable of exerting an inhibition on the protein and its protein complexes (Blumenthal et al., 1988).

A direct detection tool developed by our group is the calmodulin biosensor (*h*CaM-M124C-*mBBr*), which we have used to detect the binding of various ligands, This biosensor has a high sensitivity ($\phi = 0.49$) compared to CaM WT ($\phi = 0.025$) (González-Andrade et al., 2009; González-Andrade et al., 2013). On the other hand, theoretical computational studies such as Molecular Dynamics (MD) (González-Andrade et al., 2016), these are simulations that allow all the atoms in a system to vibrate and move for some time, integrating Newton's equations of motion, under a potential empirical field that approximates the energies of molecular systems

representing atoms as charged spheres and bonds as springs with defined properties. Systems have been parameterized so that they can predict the statistical properties of physicochemical systems while providing detailed information on the interactions in the system. In other words, they provide information on the conformation and stability of biological systems in solution; in our case, the $(Ca^{+2})_{0\text{-}4}$-CaM-peptide interaction.

We aimed to study the implications of different calcium equivalents on the affinity of four representatives CaM peptides (Calspermin, CaV1.1, nNOS, and skMLCK), using *h*CaM-M124C-*mBBr* and molecular modeling tools. The experimental results showed a directly proportional relationship between the degree of calcium saturation and the increased affinity of three of the four peptides studied for CaM. On the other hand, the theoretical results indicate that the saturation of calcium ions increases the degree of conformational flexibility in the Holo-CaM (higher Root Mean Square Deviation -RMSD-). At the same time, the $(Ca^{2+})_4$-CaM-Peptide complexes show appreciable conformational stability compared to the closed $(Ca^{2+})_4$-CaM (without ligands). Theoretical energy parameters show a negative theoretical ($-\Delta G_T$) in all complexes, with the enthalpy component contributing the most. The experimental and theoretical results complement each other appropriately and they can help to understand how CaM can modulate a great variety of proteins in different environments with specificity depending on the calcium concentration.

2. Materials and methods

2.1. Biosensor, peptides and reagents

The biosensor (*h*CaM M124C-*mBBr*) was obtained using the methodology described above by González-Andrade, M., and *col*. (González-Andrade et al., 2009). The peptides were acquired from the chemical peptide synthesis service of GenScript Corporation (GenScript, Piscataway, NJ, USA). All the peptides were delivered lyophilized with a purity $>$ 95%; the certificate of analysis by mass spectroscopy showed the following sequences Calspermin (ARRKLKAAVKAVVASSRLGS), CaV1.1 (KFYATFLIQEHFRKFMKRQEE), nNOS (KRRAIGFKKLAEAV KFSAKLMGQ), and skMLCK (KRRWKKNFIAVSAANRFKKISSSGAL). All other reagents were of analytical reagent grade and were purchased from Sigma (St. Louis, MO) and Santa Cruz Biotechnology, Inc. (Dallas, Texas, USA).

2.2. Steady-state fluorescence

All measurements were conducted with an ISS–PC1 spectrofluorometer (ISS, Champaign, IL) with sample stirring at 37 °C. The *h*CaM M124C-*mBBr* (5 μM) was incubated in a buffer (50 mM Tris-HCl buffer, pH 7.5). Fluorescence emission spectra were acquired with excitation and emission slit widths of 4 and 8 nm, respectively. The excitation wavelength was 381 nm, and emission wavelengths of 415 to 550 nm were measured. The fractional degree of saturated *h*CaM M124C-*mBBr* with ligand (y) was calculated by changes in fluorescence on ligand binding according to $y = (F\text{-}F_0)/(F_\infty\text{-}F_0)$, where F_∞ represents the fluorescence intensity at saturation of the ligand, y is plotted as a function of the protein/ligand relation (L), and the apparent dissociation constants (K_d) and stoichiometric (S) were obtained by fitting to the equation:

$$y = \frac{(1 + K_d/S + L/S) - \sqrt{(1 + K_d/S + L/S)^2 - 4L/S}}{2} \quad (1)$$

where y represents the fractional degree of fluorescence intensity at 470 nm, K_d is the apparent dissociation constant for the ligands, L is the protein/ligand relation and S is the stoichiometric. The data were analyzed using the OriginPro version 9.1 64-bit SR2 program (OriginLab, Northampton, MA).

2.3. Preparation of initial coordinate files

The coordinates corresponding to the structure of CaM were obtained from the Protein Data Bank (PDB, http://www.rcsb.org). The structure used for the DM with different calcium was Holo-CaM (1CLL.pdb) refined at 1.7 Å (Chattopadhyaya et al., 1992) and the closed form for the $(Ca^{2+})_4$-CaM-nNOS; 2O60.pdb, refined at 1.55 Å, $(Ca^{2+})_4$-CaM-CaV1.1; 2VAY.pdb, refined at 1.94 Å (Halling et al., 2009), and $(Ca^{2+})_4$-CaM-skMLCK; 2BBM.pdb solution NMR (Ikura et al., 1992) complexes. The MD with different calcium equivalents started from the Holo-CaM structure and the corresponding calcium was progressively extracted before starting the simulation. The $(Ca^{2+})_4$-CaM-Calspermin complex was built from the 2O60.pdb structure and the Calspermin peptide, this last was modeled using MODELLERv9.2 (Webb & Sali, 2014), taking as a template the Calcineurin peptide extracted from the 2JZI.pdb structure. All the structures had the hydrogens removed before the initial preparation of the MD.

2.4. Molecular dynamics simulation

All the structural complexes were verified, cleaned, and ordered with the *pdb4amber* scrip before starting the preparation in order to generate suitable topologies from the *LEaP* module of AMBER 19 (Case et al. 2005; Case et al. 2005; D.A. Case 2012; D.A. Case et al., 2015). Each structure and complex were subjected to the following protocol: hydrogen's and other missing atoms were added using the *LEaP* module with the *leaprc.protein.ff19SB* parameter set, K^+ counterions were added to neutralize the system, the complexes were then solvated in an octahedral box of explicit *TIP3P* model water molecules localizing the box limits at 12 Å from the protein surface. MD simulations were performed at 1 atm and 315 K, maintained with the Berendsen barostat and thermostat, using periodic boundary conditions and particle mesh Ewald sums (grid spacing of 1 Å) for treating long-range electrostatic interactions with a 10 Å cutoff for computing direct interactions. The *SHAKE* algorithm was used to satisfy bond constraints, allowing the employment of a two femtoseconds time step for the integration of Newton's equations as recommended in the AMBER package (Walker et al., 2008; D.A. Case 2012). AMBER leaprc.protein.ff19SB force field (Tian et al., 2020) parameters were used for all residues. All calculations were made using graphics processing units (GPU) accelerated MD engine in AMBER (*pmemd.cuda*), a

program package that runs entirely on CUDA-enabled GPUs (Salomon-Ferrer et al., 2013b). The protocol consisted of performing a minimization of the initial structure, followed by 2500 heating steps (50ps) and pressure equilibration (50ps) at 315 K and 1.0 atm pressure, respectively. Finally, the system is equilibrated with 250,000 steps (500ps) before starting the production of MD. The production of the MD consisted of 100 ns (50,000,000 steps) for each complex. Frames were saved at ten ps intervals for subsequent analysis.

2.5. Trajectory analysis

All analyzes were done using *CPPTRAJ* part of *AMBER19* utilities and OriginPro 9.1. The calculations of RMSD and Root Mean Square Fluctuations (RMSF) were made, taking into account the atoms of C, CA, and N; for the distances, only the atoms of CA were used (Roe & Cheatham, 2013). The charts were built with OriginPro 9.1, and the trends were adjusted with the function processing smooth (method lowess span). VMD and PyMOL (DeLano, 2004) were used to visualize and create the images from the MD.

2.6. Binding free energies calculated by molecular mechanics/poisson boltzmann surface area (MM/PBSA)

This method involves a combination of molecular mechanic's energy with implicit solvation models to calculate binding free energies. In *MM/PBSA.py* (Zhou & Madura, 2004), binding free energy (ΔG_{bind}) between a ligand (L) and a target (T) to form a complex is calculated as:

$$\Delta G_{bind} = \Delta H - T\Delta S \approx \Delta E_{MM} + \Delta G_{Sol} - T\Delta S$$
$$\Delta E_{MM} = \Delta E_{Internal} + \Delta E_{Electrostatic} + \Delta E_{Vdw}$$
$$\Delta G_{Sol} = \Delta G_{PB} + \Delta G_{SA}$$

where ΔE_{MM}, ΔG_{Sol}, and $-T\Delta S$ are the changes of the gas phase molecular mechanics energy, the solvation free energy, and the conformational entropy upon binding, respectively. ΔE_{MM} comprises $\Delta E_{Internal}$ (bond, angle and dihedral energies), $\Delta E_{Electrostatic}$ (electrostatic energies), and ΔE_{Vdw} (van der Waals energies). ΔG_{Solv} is the sum of electrostatic solvation energy (polar contribution) -ΔG_{PB}- and non-electrostatic solvation component (non-polar contribution) -ΔG_{SA}-. The polar contribution is calculated using the Poisson-Boltzmann surface area model, while the non-polar energy is estimated from the solvent-accessible surface area (*SASA*). The conformational entropy change (-$T\Delta S$) was computed by normal mode analysis from a set of conformational snapshots taken from the MD simulations (Hou et al., 2011; Kollman et al., 2000).

3. Results and discussion

3.1. CaM titration with calcium

Proteins are generally surrounded by possible ligands (proteins, cations, organic molecules, water, etc.) with different properties. However, most proteins are specific for their ligand; but some have more than one ligand and establishing interactions with proteins to regulate various cellular processes, such is the case of the CaM.

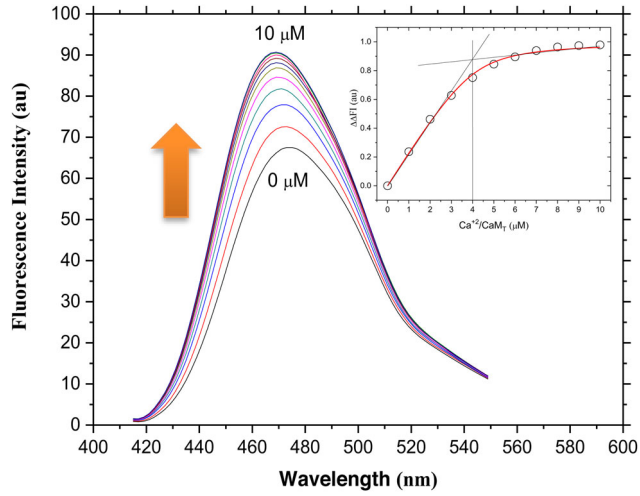

Figure 2. Fluorescence spectra and Ca^{+2} titration curve with the *h*CaM-M124C-*mBBr* biosensor. The spectra were obtained by exciting the CaM biosensor with λ_{exc}=381 nm, in an emission interval λ_{emi}=405-550 nm. Using a 1 mM $CaCl_2$ solution and a concentration of 5 μM of *h*CaM-M124C-*mBBr*, in 50 mM Tris-HCl buffer, pH 7.5 at 37 °C. The inset-graph shows the change in fluorescence intensity as a function of the added Ca^{+2}/CaM molar ratio, adjusted to a second-order equation, (*see materials and methods*).

The formation of the (Ca^{+2})-CaM complex with different calcium equivalents is a mechanism by which CaM can regulate a wide variety of functions, through many proteins; various research groups have studied the kinetic behavior of Ca^{+2} on CaM, determining the stoichiometry and K_{ds} of the calcium ion according to the sites of the union of this (Persechini & Stemmer, 2002). The binding of calcium to CaM has been well described as a sequential and ordered model; therefore, it is assumed that each binding site has structural and functional characteristics in CaM. This model describes an asymmetry of the CaM in the Apo form, where site III has the highest affinity and once calcium binds, conformational changes are triggered that affect the remaining three sites; providing them with different affinities (with the following order of sites occupancy: site III→site IV→site I→site II) (Dagher et al., 2011; Gilli et al., 1998; Kilhoffer et al., 1992).

Figure 2 shows the titration of CaM with Ca^{+2}; the biosensor presents an increase in fluorescence intensity with increasing calcium concentration. This increase can be attributed to the conformational change that the CaM presents from its Apo-CaM form to Holo-CaM; since the microenvironment where the *mBBr* fluorophore (Met124) is found becomes more hydrophobic (*SASA* from 127.11 to 119.14 Å). The binding parameters obtained were a K_d = 0.244 ± 0.03 μM with a stoichiometry of 4.1 ± 0.15, literature-like values (Helassa et al., 2015). With this value, we estimate the corresponding equivalents for each calcium-binding site, considering that there may be a population average of the CaM with 1, 2, 3, and 4 calcium.

3.2. Titration of the peptides with the biosensor hCaM-M124C-mBBr with different calcium equivalents

Titrations of the Calspermin, CaV1.1, nNOS, and skMLCK peptides were performed with the biosensor *h*CaM-M124C-*mBBr*,

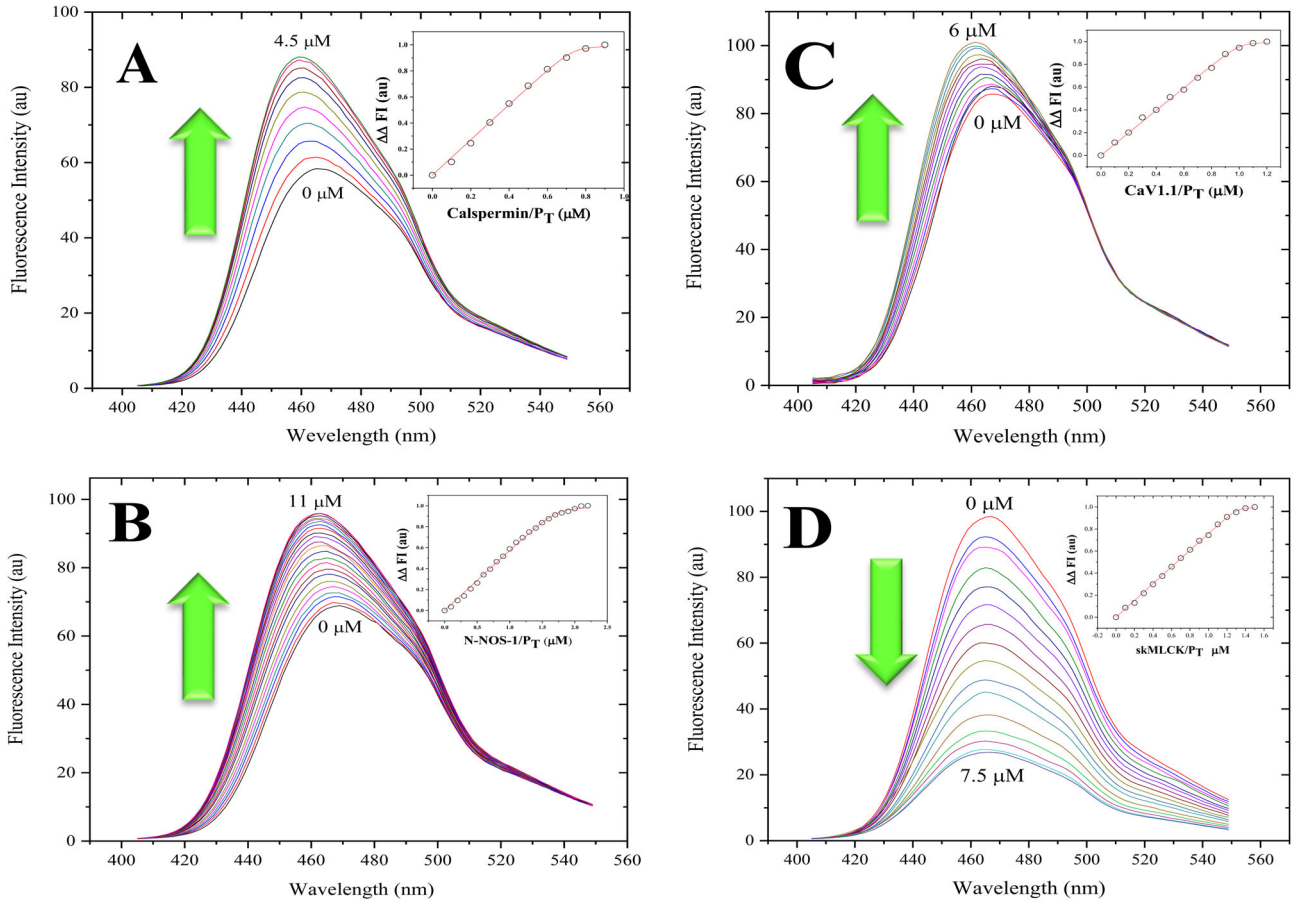

Figure 3. Fluorescence spectra and titration curves of peptides A) Calspermin, B) CaV1.1, C) nNOS, and D) skMLCK with the biosensor *h*CaM-M124C-*mBBr*. The spectra were obtained by exciting the biosensor with a λ_{exc} = 381 nm and an emission interval λ_{emi} = 405-550 nm. Using, 5 µM of the biosensor *h*CaM-M124C-*mBBr*, in 50 mM Tris-HCl buffer, pH 7.5 at 37 °C. The insets-graphics show the titration of the peptides; the solid line in red color shows the adjustment made.

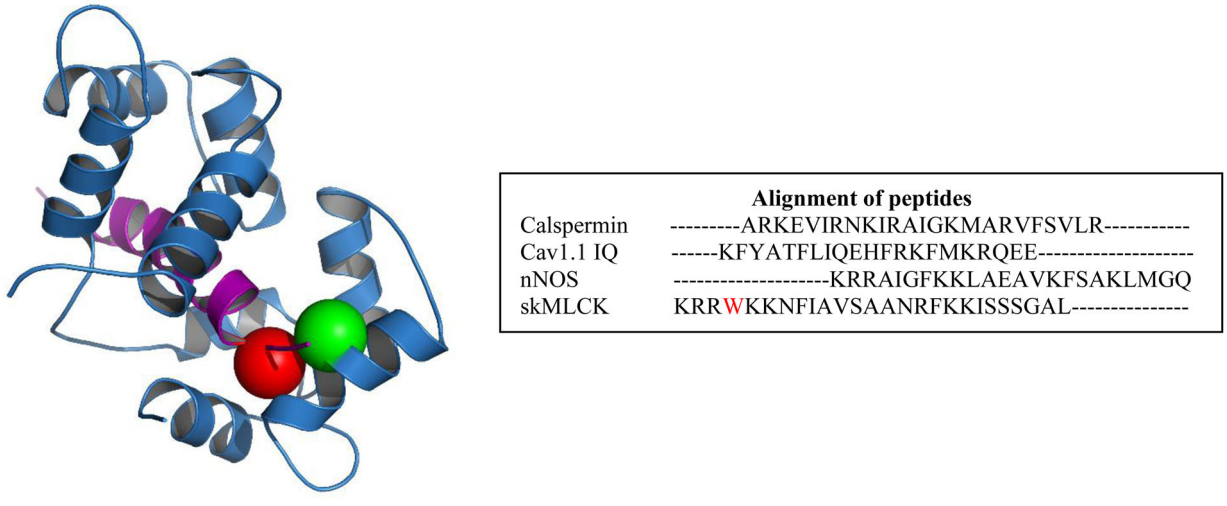

Figure 4. Interaction of the $(Ca^{2+})_4$-CaM-skMLCK complex. The three-dimensional model of the interaction of the TRP residue of the skMLCK peptide (red sphere) with the *mBBr* fluorophore of the CaM protein (green sphere) and sequential alignment of the four peptides, where the only TRP of the skMLCK peptide is observed in red. Peptide alignment was performed with Constraint-based Multiple Alignment Tool (https://www.ncbi.nlm.nih.gov/tools/cobalt/re_cobalt.cgi).

using four different calcium equivalents. One of the advantages of using this biosensor is that it can monitor more than one ligand at a time; in this case, the calcium ion and the peptides. Figure 3 shows the fluorescence spectra and the titration curves for the $(Ca^{2+})_4$-CaM-Peptide complexes, the titrations with the different calcium equivalents are presented in Figure 1S-4S (supplementary material). The addition of Calspermin, CaV1.1, and nNOS peptides to the biosensor shows an increase in fluorescence intensity (hyperchromic effect). However, the skMLCK peptide causes a decrease in it (hypochromic effect). The change in fluorescence intensity of the biosensor used is attributed to the extrinsic fluorescence of the fluorophore monobromobimane (*mBBr*), which respond to the change in the microenvironment generated

Table 2. Determination of dissociation constants of peptides with different equivalents of Ca^{2+}, using the biosensor *h*CaM-M124C-*mBBr*.

Peptide/Ca^{2+}	0.0 Equiv	1.0 Equiv	2.0 Equiv	3.0 Equiv	4.0 Equiv
			K_d (nM)		
Calspermin	32.3 ± 7.4	27.4 ± 7.6	9.9 ± 3.9	10.2 ± 4.9	2.4 ± 1.6
Cav1.1	1.5 ± 2.0	1.9 ± 2.1	1.9 ± 1.4	2.5 ± 0.9	1.9 ± 1.3
nNOS	84.7 ± 17.6	47.7 ± 10.3	34.0 ± 8.8	9.6 ± 1.7	10.2 ± 1.2
skMLCK	43.2 ± 13.8	39.7 ± 8.9	9.1 ± 6.0	3.3 ± 1.8	1.4 ± 0.7
			Stoichiometry		
Calspermin	0.87 ± 0.3	0.81 ± 0.3	0.81 ± 0.3	0.81 ± 0.2	0.93 ± 0.1
Cav1.1	1.06 ± 0.02	1.02 ± 0.03	1.13 ± 0.02	1.14 ± 0.01	1.0 ± 0.01
nNOS	1.5 ± 0.81	1.5 ± 0.54	1.25 ± 0.48	1.3 ± 0.52	1.7 ± 0.20
skMLCK	0.79 ± 0.21	0.68 ± 0.34	0.97 ± 0.18	1.09 ± 0.15	1.31 ± 0.22

by the binding of the peptides. The structural analysis of the interactions between (Ca^{2+})-CaM and the peptides indicate that the union of these generates a hydrophobic microenvironment at position 124 of the CaM, where it is chemically labeled with the fluorophore. In the case of the skMLCK peptide, it has a tryptophan residue at position 4, which interacts directly with position 124, where the *mBBr* is located, producing a quenching effect (Figure 4). This effect for the $(Ca^{2+})_4$-CaM-skMLCK complex, had previously been reported by Hans J. Vogel *et al*., where they perform mutagenesis in methionine residues that are in the C-Terminal domain of CaM by selenomethionine or leucine and observe the quenching of the tryptophan of the peptide (Weljie & Vogel, 2000; Yuan et al., 1998).

Table 2 shows the binding parameters obtained for each peptide with their respective calcium equivalents. The Calspermin, nNOS, and skMLCK peptides show a higher affinity based on the number of calcium equivalents, CaV1.1 shows an affinity independent of calcium equivalents. All the peptides studied have an affinity in the nanomolar range and a binding stoichiometry around 1.0, which is expected and validates the fit model used (*see Material and methods*). The increase in affinity from apo-CaM to Holo-CaM is 13.4, 8.3, and 30.8 times for the Calspermin, nNOS, and skMLCK peptides, respectively.

The K_{ds} calculated for the Calspermin peptide are in the range of 32 to 2 nM for the $(Ca^{2+})_{0\text{-}4}$-CaM-Calspermin complexes. Previous reports for the $(Ca^{2+})_4$-CaM-Proteín-Calspermin complex reported a $K_d = 4.42$ nM using surface plasmon resonance (SPR) (Murphy et al., 2008). For the CaV1.1 peptide, the K_{ds} obtained with the CaM biosensor are around 2 nM, unrelatedly of the number of calcium equivalents. Cav1.1 channel are proteins that are almost exclusively expressed in skeletal muscle cells. A mechanical link transmits the conformational changes in the voltage-sensing domains in Cav1.1 to the associated ryanodine receptors, which release Ca^{2+} from the sarcoplasmic reticulum. CaM mediates Ca^{2+} dependent inactivation (CDI) to binding to the C-Terminus of the CaV1.1 protein (Catterall et al., 2005; Stockner & Koschak, 2013). Three domains have been identified within this region: I) an EF binding motif binding Ca^{2+}, II) a CaM binding site, and III) an IQ CaM binding motif (Stroffekova, 2011; Tang et al., 2003; Tidow & Nissen, 2013). The Ca^{2+}-CaM complex binds to the IQ motif, which corresponds to the CaV1.1 peptide (Tang et al., 2003). CDI is likely responsible for the CaV1.1 peptide showing a calcium-independent affinity in titrations with the biosensor *h*CaM-M124C-*mBBr*. The nNOS peptide shows a calcium-dependent affinity, the calculated K_{ds} range is from 84 nM (CaM-nNOS) to 10 nM ($(Ca^{2+})_4$-CaM-nNOS); for the nNOS peptide, $K_d = 2.2$ nM obtained by enzymatic inhibition assay and K_d between 0.8-3.9 nM using SPR have been reported (Zhang & Vogel, 1994). The skMLCK peptide has the highest affinity variation (K_{ds}) between the CaM-skMLCK and $(Ca^{2+})_4$-CaM-skMLCK complex, around 30 times (K_{ds} from 43.2 to 1.4 nM), previous reports calculate a $K_d = 1.0$ nM at calcium saturation (Lukas et al., 1986).

3.3. Molecular dynamics of CaM with different calcium equivalent

MD of the CaM structure was carried out by varying the calcium ions (0-4 calcium). Figure 5 shows the conformations it adopts the CaM along with the DM; and the RMSD as a function of time. The RMSD is a parameter that allows us to discretely evaluate the fluctuations between each fragment of MD, which is why it reflects the conformational stability of the system. In the absence of calcium, the conformational stability is maintained (RMSD ~5 Å); and while more calcium sites are occupied, the RMSD increases around 13-14 Å. For the $(Ca^{2+})_3$-CaM and $(Ca^{2+})_4$-CaM complex, a more significant conformational fluctuation is observed. By extrapolating these results to the functional part, CaM being a very flexible protein, its multispecific properties may be related to the degree of flexibility, and the ability to adopt more conformations is, in turn, modulated by the number of cations that bind to it. In this experiment, we start from the saturated calcium structure -$(Ca^{2+})_4$-CaM)-, to which we eliminated the calcium and subjected it to MD. The absence of calcium makes the protein maintain its overall structural stability as there are subtle local changes. However, the same structure (Holo-CaM) with more cations shows greater conformational flexibility. The latter leads us to speculate that CaM is modulated by calcium ions to acquire greater mobility and thus be able to interact with higher probability with specific ligands. Another important aspect is the intramolecular communication caused by the ions in the CaM since by gradually binding, these could interfere with the affinity of the remaining calcium-binding sites.

Another parameter used to analyze MD trajectories is the RMSF, which indicates the degree of displacement of a set of atoms corresponding to a residue with respect to a reference. Figure 6 shows the RMSF about the number of residues, the range obtained for all the MDs of the CaM with different calcium's is from 2 to 13 Å. Overall, it is observed that the residues corresponding to the loops that some coincide with the residues involved in the calcium-binding sites have a higher RMSF. The lobe corresponding to the C-Terminal (90-148), presents greater conformational flexibility, this argument coincides with data previously explored by other authors for this system (Smith et al., 2012).

3.4. Molecular dynamics of CaM-Peptide complexes

MD of all the CaM-peptide complexes studied in this work was performed with and without calcium, for 100 ns since the binding energy analyzes show that from 60 ns, the

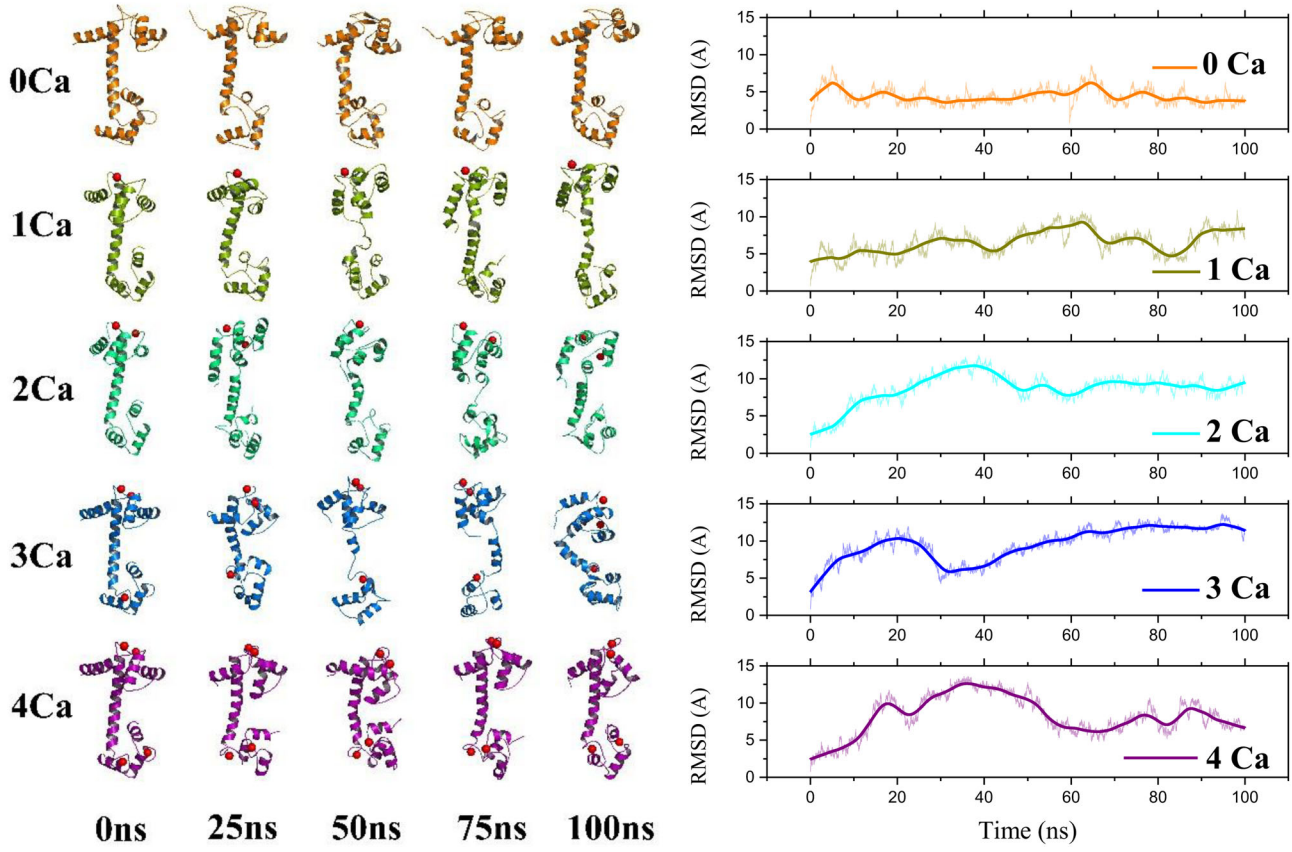

Figure 5. Structures and RMSD of the MD of Holo-CaM with different calcium equivalents. The structures obtained every 25 ns are shown on the left. Calcium ions are shown in red spheres, CaM orange cartoons, $(Ca^{2+})_1$-CaM green cartoons, $(Ca^{2+})_2$-CaM cyan cartoons, $(Ca^{2+})_3$-CaM blue cartoons, and $(Ca^{2+})_4$-CaM purple cartoons. The structure used to perform the MD corresponds to Holo-CaM (1CLL.pdb). The analyzes and figures were made with CPPTRAJ (Roe & Cheatham, 2013), OriginPro 9.1, and PyMOL (DeLano, 2004).

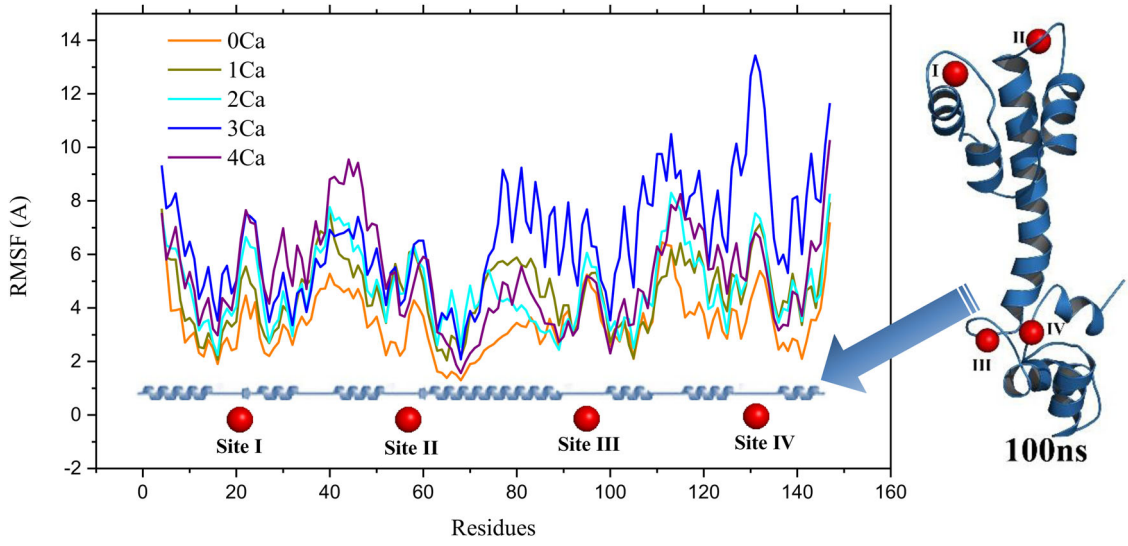

Figure 6. RMSF vs Holo-CaM residue in binding to different Ca^{2+} during 100 ns of MD. The structural model on the right corresponds to the $(Ca^{2+})_4$-CaM complex at the beginning and end of the MD.

differences are not significant (Figure 5(A) and Table 1s). Using this tool allows us to analyze molecular-level details of Protein-Peptide interactions, predict theoretical binding energy (ΔG_T), and analyze systems as a function of time. The simulation comprises five stages: I) Minimization, II) Heating, III) Pressure equilibration, IV) Equilibrium, and V) Production of the system, where it is intended to maintain thermodynamic equilibrium conditions similar to the experimental (Case et al. 2005; González-Andrade et al., 2016; Salomon-Ferrer et al., 2013a). The data obtained from these MD is used to compare and complement with the experimental results. Figure 7 shows the structural models every 25 ns of MD of the four $(Ca^{2+})_4$-CaM-Peptide complexes and the closed conformation of the $(Ca^{2+})_4$-CaM (without

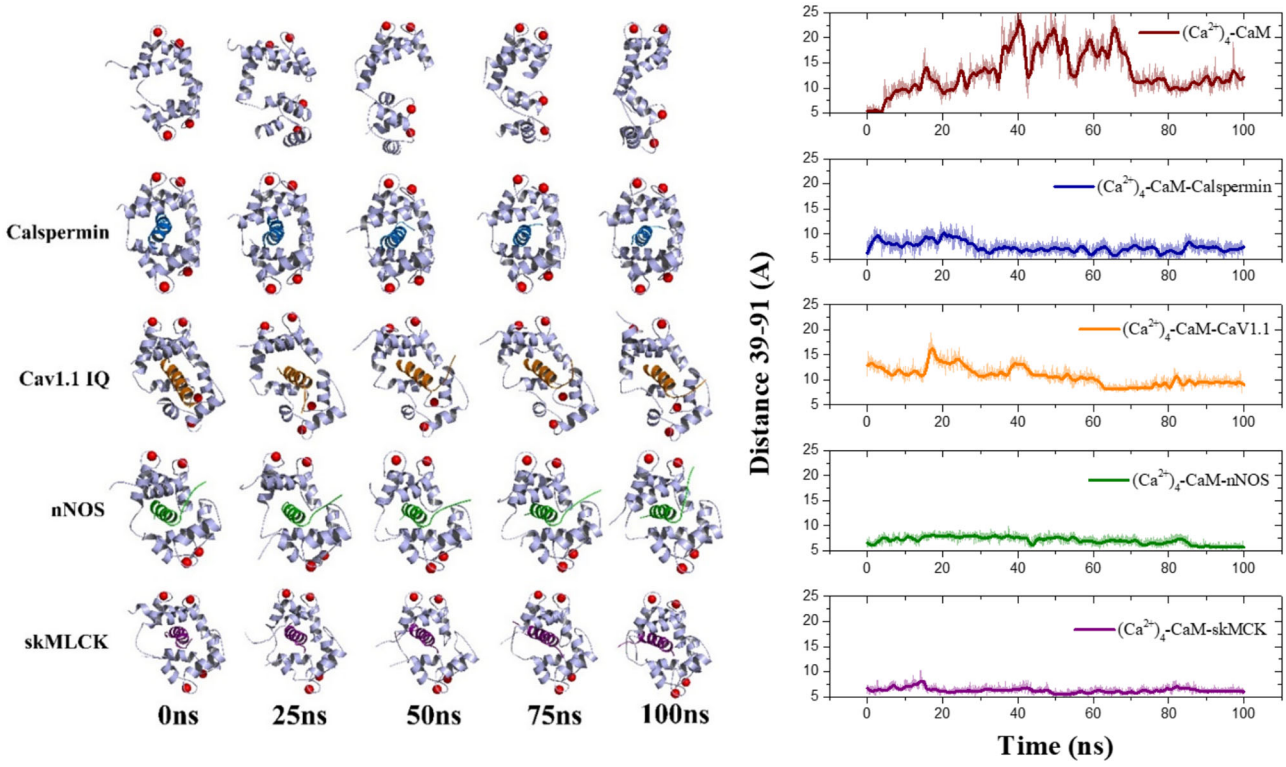

Figure 7. Structural models and distances between CaM lobes in $(Ca^{2+})_4$-CaM-peptides complexes from 0-100ns of MD. The structures used in the simulation correspond to the closed form; 2060.pdb for $(Ca^{2+})_4$-CaM and the nNOS and Calspermin peptides; 2VAY.pdb for CaV1.1 peptide and 2BBM.pdb for skMLCK peptide. The analyzes and figures were made with CPPTRAJ (Roe & Cheatham, 2013), OriginPro 9.1, and PyMOL (DeLano, 2004).

peptide). The visual results of the four complexes show appreciable conformational stability compared to $(Ca^{2+})_4$-CaM in the closed state without peptide, where the latter fluctuates and tends to open. One way to analyze conformational stability was by measuring the opening of the CaM, through the distance between the strategically chosen residues 39 and 91, located in each lobe of the protein. These residues had previously been used by our working group to develop fluorescent biosensors (González-Andrade et al., 2011). The distances for closed $(Ca^{2+})_4$-CaM without peptide fluctuate between 4.5 and 27.8 Å, while for $(Ca^{2+})_4$-CaM-Calspermin (3.6-12.23 Å), $(Ca^{2+})_4$-CaM-CaV1.1 (7.2-19.2 Å), $(Ca^{2+})_4$-CaM-nNOS (5.0-9.8 Å), and $(Ca^{2+})_4$-CaM-skMLCK (4.7-10.1 Å) complexes. The complexes are corresponding to the Calspermin, nNOS, and skMLCK peptides average 10.7 Å as the maximum opening distance, and for the CaV1.1 peptide, this shows a maximum distance of 19.2 Å. These distances can indirectly illustrate the degree of conformational stability exhibited by the complexes from the stage of production of MDs. However, a qualitative way to analyze the degree of binding of peptides to CaM is through a normal mode analysis of the interaction of CaM-Peptides complexes.

Table 3 shows the results obtained from the analysis in normal modes of the complexes without calcium and with the four occupied sites, broken down into theoretical ΔG_T, ΔH_T, and ΔS_T. The ΔG_T was compared with the experimental ΔG (ΔG_E), the latter obtained from *K*ds. The goal of performing the MDs of the complexes with and without calcium arose from the experimental results, to see if the simulations of MD were able to discern this condition. In all cases, the calcium complexes showed a lower ΔG_T, which is in harmony with the experimental data. The difference between the value of ΔG_E and ΔG_T is 30-40 kcal mol^{-1} in the complexes, although this difference is significant to compare and analyze quantitatively; if we can try to extrapolate qualitative information. For example, the most negative ΔG_T corresponds to the $(Ca^{2+})_4$-CaM-Calspermin (-58.51 kcal mol^{-1}) and $(Ca^{2+})_4$-CaM-skMLCK (-58.38 kcal mol^{-1}) complex, and these present the highest affinities in this same condition K_d=2.4 and K_d=1.4 nM, respectively. Another data to highlight is the value of the ΔG_T obtained (between −32.26 and −58.51 kcal mol-1) for the $(Ca^{2+})_4$-CaM-peptide complexes, being more negative values compared to data previously reported for $(Ca^{2+})_4$-CaM-Drugs using the same simulation algorithm (AMBER) (González-Andrade et al., 2016).

We compared the RMSD of the CaM-Peptide complexes with and without calcium, along with the closed state $(Ca^{2+})_4$-CaM without peptide. Figure 8, shows the results obtained, where we can visualize that there is a difference of at least 10 Å of RMSD between the $(Ca^{+2})_4$-CaM-Peptide and $(Ca^{+2})_4$-CaM (closed) complexes; this allows us to discern that the union of the peptides structurally stabilizes the CaM. While $(Ca^{2+})_4$-CaM in the closed state without ligand tends to open, in the same way that the Holo-CaM tries to close, which follows that the protein is in constant movement between one state and another. Another interesting data is that the RMSDs of the CaM-Pepetido complex with and without calcium is slightly different, where the four calcium complexes have a higher RMSD and less fluctuation between each step of the dynamics. The fluctuation observed between each step of the dynamics may be reflecting the optimal energy search of the complexes. It should be noted

Table 3. Results obtained from the binding of the Calspermin, CaV1.1, nNOS, and skMLCK peptides to the CaM.

	Experimental		Theoretical[3]		
Complex	K_d[1] (nM)	ΔG_{Exp}[2] (kcal/mol)	ΔG_{tThe} (kcal/mol)	ΔH_{The} (kcal/mol)	$T\Delta S_{The}$ (kcal/mol)
CaM-Calspermin	32.3 ± 7.4	−10.21	−55.77 ± 4.8	−125.34 ± 3.5	−69.59 ± 6.3
$(Ca^{2+})_4$-CaM-Calspermin	2.4 ± 1.6	−11.75	−58.51 ± 5.8	−132.38 ± 4.5	−73.87 ± 4.1
CaM-Cav1.1	1.5 ± 2.0	−12.03	−32.26 ± 1.2	−92.80 ± 6.6	−60.53 ± 7.3
$(Ca^{2+})_4$-CaM-Cav1.1	1.9 ± 1.3	−11.89	−38.78 ± 8.2	−101.32 ± 9.6	−62.58 ± 7.3
CaM-nNOS	84.7 ± 17.6	−6.41	−34.80 ± 6.5	−110.4 ± 8.7	−75.69 ± 6.8
$(Ca^{2+})_4$-CaM-nNOS	10.2 ± 0.2	−10.90	−37.54 ± 7.2	−120.45 ± 9.9	−82.9 ± 7.0
CaM-skMLCK	43.2 ± 13.8	−10.04	−48.00 ± 8.9	−127.63 ± 15.0	−79.63 ± 6.5
$(Ca^{2+})_4$-CaM-skMLCK	1.4 ± 0.7	−12.07	−58.35 ± 9.6	−153.42 ± 11.4	−95.07 ± 7.2

[1]Experimentally determined apparent dissociation constant for the CaM-peptide and $(Ca^{2+})_4$-CaM-peptide complex.
[2]Gibbs energy obtained from the experimental apparent dissociation constant using the equation $\Delta G^{\circ} = -RT \ln k_d$, where $R = 1.987 \times 10^{-3}$ kcal/mol*K and $T = 298.15$ K.
[3]Results obtained from a simulation of 100 ns of MD for the CaM-peptide and $(Ca^{2+})_4$-CaM-peptide complexes using the MM/PBSA.py normal mode analysis method.

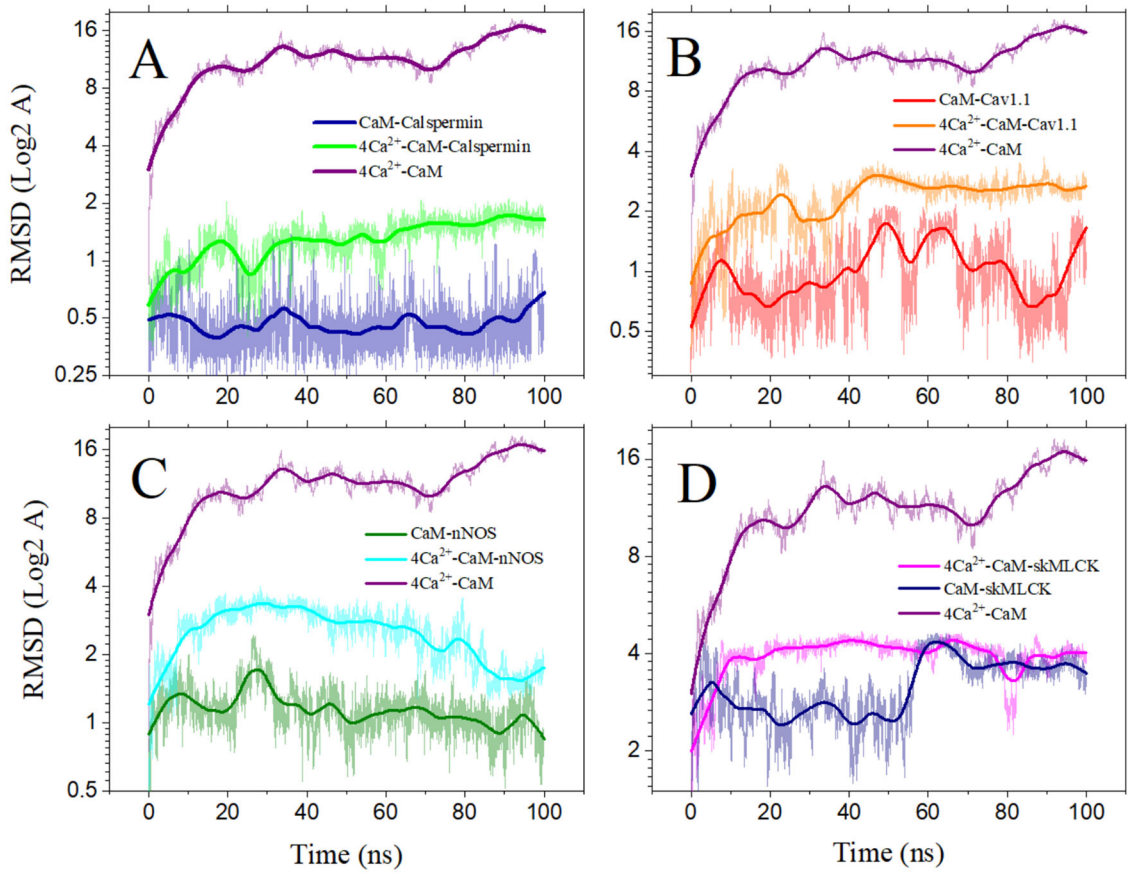

Figure 8. RMSD as a function of time of the CaM-pepdido complexes in closed conformation with and without calcium. A) CaM-Caspermin, B) CaM-Cav1.1, C) CaM-nNOS, and D) CaM-skMLCK. The scale corresponding to the RMSD is shown in Log2 for a better appreciation. The analyzes and figures were made with CPPTRAJ [75] and OriginPro 9.1.

that the simulation of MD in this system has around 33442 atoms (2704, 4, 8 and 30726 atoms of the complex, Ca^{2+}, eight counterions, and waters, respectively) and the only difference between the CaM-Peptide and $(Ca^{2+})_4$-CaM-peptides complexes are four calcium atoms (0.011%).

4. Conclusions

The CaM protein from the biological point of view is a versatile and multifunctional system that regulates functions in different cellular compartments where there are different concentrations of calcium. In this work, we focus on the study of the CaM-Peptide interaction by varying the calcium equivalents in the complex experimentally and theoretically, using the *h*CaM-M124C-*mBBr* biosensor and molecular modeling tools. Due sensitivity of the biosensor, we were able to establish four calcium equivalents until saturating the CaM and with this, being able to titrate the peptides, obtaining five K_{ds}. Three of the four peptides studied showed a relationship directly proportional to the number of Ca^{2+} equivalent concerning its affinity, while the affinity of the CaV1.1 peptide was independent of calcium. All the peptides have K_d in the nM range in order of magnitude less than most of the drugs and ligands previously reported for CaM. On the

other hand, the MD studies were designed based on the experimental results were in the first instance we analyzed the implications of gradually removing a calcium ion from the Holo-CaM, where we visualize that this progressive elimination reduces its conformational flexibility. Another interesting data is that the CaM-Peptide complexes with and without calcium show subtle differences in both binding energy results (ΔG_T) and RMSD, which are in harmony with the experimental results (K_{ds} and ΔG_E). Our results demonstrate the importance of the use of highly sensitive biosensors and the power of MD to make inferences in systems such as CaM-peptide complexes; to design new peptides or ligands of CaM, taking into account the possible conformations based on the calcium equivalents that the protein can bind.

Acknowledgements

The authors are very grateful to Mrs. Maria Josefina Bolado Garza from the División de Investigación, Facultad de Medicina, UNAM for the review and edition of the manuscript. We are indebted to Dirección General de Cómputo y de Tecnologías de Información y Comunicación, UNAM, for providing the resources to carry out computational calculations through MIZTLI System.

Disclosure statement

No potential conflict of interest was reported by the author

Funding

This work was supported by grants from DGAPA-UNAM (PAPIIT-IN203719), DGTIC-UNAM (LANCAD-UNAM-DGTIC-313) and internal budget awarded from the Faculty of Medicine, UNAM.

ORCID

Martin González-Andrade http://orcid.org/0000-0002-8910-3035

References

Ataman, Z. A., Gakhar, L., Sorensen, B. R., Hell, J. W., & Shea, M. A. (2007). The NMDA receptor NR1 C1 region bound to calmodulin: Structural insights into functional differences between homologous domains. *Structure (London, England: 1993)*, *15*(12), 1603–1617. https://doi.org/10.1016/j.str.2007.10.012

Audran, E., Dagher, R., Gioria, S., Tsvetkov, P. O., Kulikova, A. A., Didier, B., Villa, P., Makarov, A. A., Kilhoffer, M.-C., & Haiech, J. (2013). A general framework to characterize inhibitors of calmodulin: Use of calmodulin inhibitors to study the interaction between calmodulin and its calmodulin binding domains. *Biochimica et Biophysica Acta (BBA) - Molecular Cell Research*, *1833*(7), 1720–1731. https://doi.org/10.1016/j.bbamcr.2013.01.008

Berridge, M. J. (1997). Elementary and global aspects of calcium signalling. *The Journal of Experimental Biology*, *200*(Pt 2), 315–319.

Blumenthal, D. K., Charbonneau, H., Edelman, A. M., Hinds, T. R., Rosenberg, G. B., Storm, D. R., Vincenzi, F. F., Beavo, J. A., & Krebs, E. G. (1988). Synthetic peptides based on the calmodulin-binding domain of myosin light chain kinase inhibit activation of other calmodulin-dependent enzymes. *Biochemical and Biophysical Research Communications*, *156*(2), 860–865.

Brini, M., & Carafoli, E. (2000). Calcium signalling: A historical account, recent developments and future perspectives. *Cellular and Molecular Life Sciences: CMLS*, *57*(3), 354–370. https://doi.org/10.1007/PL00000698

Case, D. A., Cheatham, T. E., 3rd, Darden, T., Gohlke, H., Luo, R., Merz, K. M., Jr., Onufriev, A., Simmerling, C., Wang, B., & Woods, R. J. (2005). The Amber biomolecular simulation programs. *Journal of Computational Chemistry*, *26*(16), 1668–1688. https://doi.org/10.1002/jcc.20290

Case, D. A., Cheatham, T. E., 3rd, Darden, T., Gohlke, H., Luo, R., Merz, K. M., Jr., Onufriev, A., Simmerling, C., Wang, B., & Woods, R. J. (2005). The Amber biomolecular simulation programs. *Journal of Computational Chemistry*, *26*(16), 1668–1688. https://doi.org/10.1002/jcc.20290

Case, D. A., Cheatham, T. E., Darden, T. O. M., Gohlke, H., Luo, R. A. Y., Merz, K. M., Onufriev, A., Simmerling, C., Wang, B., & Woods, R. J. (2005). The Amber biomolecular simulation programs. *Journal of Computational Chemistry*, *26*(16), 1668–1688. https://doi.org/10.1002/jcc.20290

Catterall, W. A., Perez-Reyes, E., Snutch, T. P., & Striessnig, J. (2005). International union of pharmacology. XLVIII. Nomenclature and structure-function relationships of voltage-gated calcium channels. *Pharmacological Reviews*, *57*(4), 411–425. https://doi.org/10.1124/pr.57.4.5

Chattopadhyaya, R., Meador, W. E., Means, A. R., & Quiocho, F. A. (1992). Calmodulin structure refined at 1.7 A resolution. *Journal of Molecular Biology*, *228*(4), 1177–1192.

Chen, Y. T., Chao, W. C., Kuo, H. T., Shen, J. Y., Chen, I. H., Yang, H. C., Wang, J. S., Lu, J. F., Cheng, R. P., & Chou, P. T. (2016). Probing the polarity and water environment at the protein-peptide binding interface using tryptophan analogues. *Biochemistry and Biophysics Reports.*, *7*, 113–118.

Clapperton, J. A., Martin, S. R., Smerdon, S. J., Gamblin, S. J., & Bayley, P. M. (2002). Structure of the complex of calmodulin with the target sequence of calmodulin-dependent protein kinase I: Studies of the kinase activation mechanism. *Biochemistry*, *41*(50), 14669–14679. https://doi.org/10.1021/bi026660t

Case, D. A., Berryman, J. T., Betz, R. M., Cerutti, D. S., Cheatham III, T. E., Darden, T. A., Duke, R. E., Giese, T. J., Gohlke, H., Goetz, A. W., Homeyer, N., Izadi, S., Janowski, P., Kaus, J., Kovalenko, A., Lee, T. S., LeGrand, S., Li, P., Luchko, T. … Kollman, P. A. (2015). *AMBER 2015*. University of California.

Case, D. A., Darden, T. A., Cheatham III, T. E.,, Simmerling, C. L., Wang, J., Duke, R. E., Luo, R., Walker, R. C., Zhang, W., Merz, K. M., Roberts, B., Hayik, S., Roitberg, A., Seabra, G., Swails, J., Goetz, A. W., Kolossvai, I., Wong, K. F., Paesani, F. … Kollman, P. A. (2012). *AMBER 12*. University of California.

Dagher, R., Peng, S., Gioria, S., Feve, M., Zeniou, M., Zimmermann, M., Pigault, C., Haiech, J., & Kilhoffer, M. C. (2011). A general strategy to characterize calmodulin-calcium complexes involved in CaM-target recognition: DAPK and EGFR calmodulin binding domains interact with different calmodulin-calcium complexes. *Biochimica et Biophysica Acta*, *1813*(5), 1059–1067. https://doi.org/10.1016/j.bbamcr.2010.11.004

DeLano, W. L. (2004). Use of PYMOL as a communications tool for molecular science. *Abstracts of Papers of the American Chemical Society*, *228*, U313–U314.

Elshorst, B., Hennig, M., Forsterling, H., Diener, A., Maurer, M., Schulte, P., Schwalbe, H., Griesinger, C., Krebs, J., Schmid, H., Vorherr, T., & Carafoli, E. (1999). NMR solution structure of a complex of calmodulin with a binding peptide of the Ca2+ pump. *Biochemistry*, *38*(38), 12320–12332. https://doi.org/10.1021/bi9908235

Gilli, R., Lafitte, D., Lopez, C., Kilhoffer, M., Makarov, A., Briand, C., & Haiech, J. (1998). Thermodynamic analysis of calcium and magnesium binding to calmodulin. *Biochemistry*, *37*(16), 5450–5456. https://doi.org/10.1021/bi972083a

González-Andrade, M., Rodríguez-Sotres, R., Madariaga-Mazón, A., Rivera-Chávez, J., Mata, R., Sosa-Peinado, A., Del Pozo-Yauner, L., & Arias-Olguín, I. I. (2016). Insights into molecular interactions between CaM and its inhibitors from molecular dynamics simulations and experimental data. *Journal of Biomolecular Structure & Dynamics*, *34*(1), 78–91. https://doi.org/10.1080/07391102.2015.102222525702612

González-Andrade, M., Rodríguez-Sotres, R., Madariaga-Mazón, A., Rivera-Chávez, J., Mata, R., Sosa-Peinado, A., Del Pozo-Yauner, L., & Arias-Olguín, I. I. (2016). Insights into molecular interactions between CaM and its inhibitors from molecular dynamics simulations and

experimental data. *Journal of Biomolecular Structure & Dynamics*, *34*(1), 78–91. https://doi.org/10.1080/07391102.2015.102222525702612

González-Andrade, M., Del Valle, P., Macías-Rubalcava, M. L., Sosa-Peinado, A., Del Carmen González, M., & Mata, R. (2013). Calmodulin inhibitors from aspergillus stromatoides. *Chemistry & Biodiversity*, *10*(3), 328–337. https://doi.org/10.1002/cbdv.201200321

González-Andrade, M., Figueroa, M., Rodriguez-Sotres, R., Mata, R., & Sosa-Peinado, A. (2009). An alternative assay to discover potential calmodulin inhibitors using a human fluorophore-labeled CaM protein. *Analytical Biochemistry*, *387*(1), 64–70. https://doi.org/10.1016/j.ab.2009.01.002

González-Andrade, M., Rivera-Chávez, J., Sosa-Peinado, A., Figueroa, M., Rodríguez-Sotres, R., & Mata, R., (2011). Development of the fluorescent biosensor h calmodulin (hCaM)L39C- monobromobimane(mBBr)/V91C-mBBr, a novel tool for discovering new calmodulin inhibitors and detecting calcium. *Journal of Medicinal Chemistry*, *54*(11), 3875–3884. https://doi.org/10.1021/jm200167g

González-Andrade, M., Rodriguez-Sotres, R., Madariaga-Mazon, A., Rivera-Chavez, J., Mata, R., Sosa-Peinado, A., del Pozo-Yauner, L., & Arias-Olguin, I. I. (2016). Insights into molecular interactions between CaM and its inhibitors from molecular dynamics simulations and experimental data. *Journal of Biomolecular Structure & Dynamics*, *34*(1), 78–91. https://doi.org/10.1080/07391102.2015.1022225

Grishaev, A., Anthis, N. J., & Clore, G. M. (2012). Contrast-matched small-angle X-ray scattering from a heavy-atom-labeled protein in structure determination: Application to a lead-substituted calmodulin-peptide complex. *Journal of the American Chemical Society*, *134*(36), 14686–14689. https://doi.org/10.1021/ja306359z

Halling, D. B., Georgiou, D. K., Black, D. J., Yang, G., Fallon, J. L., Quiocho, F. A., Pedersen, S. E., & Hamilton, S. L. (2009). Determinants in CaV1 channels that regulate the Ca2+ sensitivity of bound calmodulin . *The Journal of Biological Chemistry*, *284*(30), 20041–20051. https://doi.org/10.1074/jbc.M109.013326

Helassa, N., Zhang, X. H., Conte, I., Scaringi, J., Esposito, E., Bradley, J., Carter, T., Ogden, D., Morad, M., & Torok, K. (2015). Fast-response calmodulin-based fluorescent indicators reveal rapid intracellular calcium dynamics. *Scientific Reports*, *5*, 15978. https://doi.org/10.1038/srep15978

Hou, T., Wang, J., Li, Y., & Wang, W. (2011). Assessing the performance of the MM/PBSA and MM/GBSA methods. 1. The accuracy of binding free energy calculations based on molecular dynamics simulations. *J Chem Inf Model*, *51*(1), 69–82. https://doi.org/10.1021/ci100275a

Ikura, M., Clore, G. M., Gronenborn, A. M., Zhu, G., Klee, C. B., & Bax, A. (1992). Solution structure of a calmodulin-target peptide complex by multidimensional NMR. *Science (New York, N.Y.)*, *256*(5057), 632–638. https://doi.org/10.1126/science.1585175

Ishida, H., & Vogel, H. J. (2006). Protein-peptide interaction studies demonstrate the versatility of calmodulin target protein binding. *Protein and Peptide Letters*, *13*(5), 455–465. https://doi.org/10.2174/092986606776819600

Jurado, L. A., Chockalingam, P. S., & Jarrett, H. W. (1999). Apocalmodulin. *Physiological Reviews*, *79*(3), 661–682. https://doi.org/10.1152/physrev.1999.79.3.661

Kilhoffer, M. C., Kubina, M., Travers, F., & Haiech, J. (1992). Use of engineered proteins with internal tryptophan reporter groups and perturbation techniques to probe the mechanism of ligand-protein interactions: Investigation of the mechanism of calcium binding to calmodulin. *Biochemistry*, *31*(34), 8098–8106. https://doi.org/10.1021/bi00149a046

Kollman, P. A., Massova, I., Reyes, C., Kuhn, B., Huo, S., Chong, L., Lee, M., Lee, T., Duan, Y., Wang, W., Donini, O., Cieplak, P., Srinivasan, J., Case, D. A., & Cheatham, T. E. (2000). Calculating structures and free energies of complex molecules: Combining molecular mechanics and continuum models. *Accounts of Chemical Research*, *33*(12), 889–897. https://doi.org/10.1021/ar000033j

Komeiji, Y., Ueno, Y., & Uebayasi, M. (2002). Molecular dynamics simulations revealed Ca2+-dependent conformational change of Calmodulin. *FEBS Letters*, *521*(1-3), 133–139.

Kuboniwa, H., Tjandra, N., Grzesiek, S., Ren, H., Klee, C. B., & Bax, A. (1995). Solution structure of calcium-free calmodulin. *Nature Structural Biology*, *2*(9), 768–776. https://doi.org/10.1038/nsb0995-768

Lukas, T. J., Burgess, W. H., Prendergast, F. G., Lau, W., & Watterson, D. M. (1986). Calmodulin binding domains: Characterization of a phosphorylation and calmodulin binding site from myosin light chain kinase. *Biochemistry*, *25*(6), 1458–1464. https://doi.org/10.1021/bi00354a041

Mata, R., Figueroa, M., González-Andrade, M., Rivera-Chavez, J. A., Madariaga-Mazon, A., & Del Valle, P. (2015). Calmodulin inhibitors from natural sources: An update. *Journal of Natural Products*, *78*(3), 576–586. https://doi.org/10.1021/np500954x

Maximciuc, A. A., Putkey, J. A., Shamoo, Y., & MacKenzie, K. R. (2006). Complex of calmodulin with a ryanodine receptor target reveals a novel, flexible binding mode. *Structure (London, England: 1993)*, *14*(10), 1547–1556. https://doi.org/10.1016/j.str.2006.08.011

Meador, W., Means, A., & Quiocho, F. (1992). Target enzyme recognition by calmodulin: 2.4 A structure of a calmodulin-peptide complex. *Science (New York, N.Y.)*, *257*(5074), 1251–1255. https://doi.org/10.1126/science.1519061

Murphy, A. J., Kemp, F., & Love, J. (2008). Surface plasmon resonance characterization of calspermin–calmodulin binding kinetics. *Analytical Biochemistry*, *376*(1), 61–72.

O'Day, D. H. (2003). CaMBOT: Profiling and characterizing calmodulin-binding proteins. *Cellular Signalling*, *15*(4), 347–354.

O'Neil, K. T., & DeGrado, W. F. (1990). How calmodulin binds its targets: Sequence independent recognition of amphiphilic alpha-helices. *Trends in Biochemical Sciences.*, *15*, 59–64.

Peersen, O. B., Madsen, T. S., & Falke, J. J. (1997). Intermolecular tuning of calmodulin by target peptides and proteins: Differential effects on Ca2+ binding and implications for kinase activation. *Protein Science : a Publication of the Protein Society*, *6*(4), 794–807. https://doi.org/10.1002/pro.5560060406

Persechini, A., & Stemmer, P. M. (2002). Calmodulin is a limiting factor in the cell. *Trends in Cardiovascular Medicine*, *12*(1), 32–37.

Rhoads, A. R., & Friedberg, F. (1997). Sequence motifs for calmodulin recognition. *FASEB Journal: Official Publication of the Federation of American Societies for Experimental Biology*, *11*(5), 331–340. https://doi.org/10.1096/fasebj.11.5.9141499

Roe, D. R., & Cheatham, T. E. (2013). PTRAJ and CPPTRAJ: Software for processing and analysis of molecular dynamics trajectory data. *Journal of Chemical Theory and Computation*, *9*(7), 3084–3095. https://doi.org/10.1021/ct400341p

Salomon-Ferrer, R., Case, D. A., & Walker, R. C. (2013). An overview of the Amber biomolecular simulation package. *Wiley Interdisciplinary Reviews: Computational Molecular Science*, *3*(2), 198–210.

Salomon-Ferrer, R., Gotz, A. W., Poole, D., Le Grand, S., & Walker, R. C. (2013). Routine microsecond molecular dynamics simulations with AMBER on GPUs. 2. Explicit solvent particle Mesh Ewald. *Journal of Chemical Theory and Computation*, *9*(9), 3878–3888. https://doi.org/10.1021/ct400314y

Smith, D. M., Straatsma, T. P., & Squier, T. C. (2012). Retention of conformational entropy upon calmodulin binding to target peptides is driven by transient salt bridges. *Biophysical Journal*, *103*(7), 1576–1584. https://doi.org/10.1016/j.bpj.2012.08.037

Stockner, T., & Koschak, A. (2013). What can naturally occurring mutations tell us about Ca(v)1.x channel function?(). *Biochimica et Biophysica Acta*, *1828*(7), 1598–1607. https://doi.org/10.1016/j.bbamem.2012.11.026

Stroffekova, K. (2011). The IQ motif is crucial for Cav1.1 function. *Journal of Biomedicine and Biotechnology*, *2011*, 1–9. https://doi.org/10.1155/2011/504649

Tang, W., Brent Halling, D., Black, D. J., Pate, P., Zhang, J.-Z., Pedersen, S., Altschuld, R. A., & Hamilton, S. L. (2003). Apocalmodulin and Ca2+Calmodulin-binding sites on the CaV1.2 channel. *Biophysical Journal*, *85*(3), 1538–1547.

Tian, C., Kasavajhala, K., Belfon, K., Raguette, L., Huang, H., Migues, A., Bickel, J., Wang, Y., Pincay, J., Wu, Q., & Simmerling, C. (2020). ff19SB: Amino-acid specific protein backbone parameters trained against quantum mechanics energy surfaces in solution. *Journal of Chemicl Theory and Computation*, *16*(1), 520–552. https://doi.org/10.1021/acs.jctc.9b00591

Tidow, H., & Nissen, P. (2013). Structural diversity of calmodulin binding to its target sites. *The FEBS Journal*, *280*(21), 5551–5565. https://doi.org/10.1111/febs.12296

Van Petegem, F., Chatelain, F. C., & Minor, D. L. (2005). Insights into voltage-gated calcium channel regulation from the structure of the CaV1.2 IQ

domain-Ca2+/calmodulin complex. *Nature Structural & Molecular Biology*, *12*(12), 1108–1115. https://doi.org/10.1038/nsmb1027

Vetter, S. W., & Leclerc, E. (2003). Novel aspects of calmodulin target recognition and activation. *European Journal of Biochemistry*, *270*(3), 404–414. https://doi.org/10.1046/j.1432-1033.2003.03414.x

Walker, R. C., Crowley, M. F., & Case, D. A. (2008). The implementation of a fast and accurate QM/MM potential method in Amber. *Journal of Computational Chemistry*, *29*(7), 1019–1031. https://doi.org/10.1002/jcc.20857

Wall, M. E., Clarage, J. B., & Phillips, G. N. (1997). Motions of calmodulin characterized using both Bragg and diffuse X-ray scattering. *Structure (London, England : 1993)*, *5*(12), 1599–1612.

Webb, B., & Sali, A. (2014). Protein structure modeling with MODELLER. *Methods in Molecular Biology (Clifton, N.J.)*, *1137*, 1–15. https://doi.org/10.1007/978-1-4939-0366-5_1

Weljie, A. M., & Vogel, H. J. (2000). Tryptophan fluorescence of calmodulin binding domain peptides interacting with calmodulin containing unnatural methionine analogues. *Protein Engineering*, *13*(1), 59–66. https://doi.org/10.1093/protein/13.1.59

Yuan, T., Weljie, A. M., & Vogel, H. J. (1998). Tryptophan fluorescence quenching by methionine and selenomethionine residues of calmodulin: Orientation of peptide and protein binding. *Biochemistry*, *37*(9), 3187–3195.

Zhang, M., & Vogel, H. J. (1994). Characterization of the calmodulin-binding domain of rat cerebellar nitric oxide synthase. *The Journal of Biological Chemistry*, *269*(2), 981–985.

Zhou, Z., & Madura, J. D. (2004). Relative free energy of binding and binding mode calculations of HIV-1 RT inhibitors based on dock-MM-PB/GS. *Proteins*, *57*(3), 493–503. https://doi.org/10.1002/prot.20223